Mechanistic Studies with 2-*C*-Methyl-D-erythritol 4-Phosphate Synthase from *Escherichia coli*†

David T. Fox and C. D. Poulter*

Department of Chemistry, University of Utah, Salt Lake City, Utah 84112

Received December 21, 2004; Revised Manuscript Received March 18, 2005

ABSTRACT: The mechanism of the reaction catalyzed by 2-*C*-methyl-D-erythritol 4-phosphate (MEP) synthase from *Escherichia coli* has been studied by steady-state and single-turnover kinetic experiments for the 1-deoxy-D-xylulose 5-phosphoric acid (DXP) analogues, 1,1,1-trifluoro-1-deoxy-D-xylulose 5-phosphoric acid (CF_3-DXP), 1,1-difluoro-1-deoxy-D-xylulose 5-phosphoric acid (CF_2-DXP), 1-fluoro-1-deoxy-D-xylulose 5-phosphoric acid (CF-DXP), and 1,2-dideoxy-D-hexulose 6-phosphate (Et-DXP). CF_3-DXP, CF_2-DXP, and Et-DXP were poor inhibitors, most likely because of the increase in steric bulk at C1 of DXP. The three analogues were also poor substrates for the enzyme. In contrast, CF-DXP was a good substrate ($k_{cat}^{CF-DXP} = 37 \pm 2\ s^{-1}$, $K_m^{CF-DXP} = 227 \pm 25\ \mu M$) for MEP synthase when compared to DXP ($k_{cat}^{DXP} = 29 \pm 1\ s^{-1}$, $K_m^{DXP} = 45 \pm 4\ \mu M$). A primary deuterium isotope effect was observed under single-turnover conditions when CF-DXP was incubated with 4*S*-[^{2}H]NADPH ($^Hk/^Dk = 1.34 \pm 0.01$), whereas no isotope effect was observed upon incubation with DXP and 4*S*-[^{2}H]NADPH ($^Hk/^Dk = 1.02 \pm 0.02$). The reaction did not exhibit burst kinetics for either substrate, indicating that product release is not rate-limiting. These studies suggest that positive charge does not develop at C2 of DXP during catalysis. In addition, the isotope effect with CF-DXP and 4*S*-[^{2}H]NADPH but not DXP indicates that the rearrangement step, which precedes hydride transfer, is rate-limiting for DXP but becomes partially rate-limiting for CF-DXP. Thus, rearrangement appears to be enhanced by substitution of a hydrogen atom in the methyl group of DXP by fluorine. These observations are consistent with a retro-aldol/aldol mechanism for the rearrangement during conversion of DXP to MEP.

Isopentenyl diphosphate (IPP)[1] and dimethylallyl diphosphate (DMAPP) are the five-carbon building blocks responsible for the biosynthesis of more than 30 000 isoprenoid compounds (*1*). The mevalonate pathway proceeding from acetyl-CoA was the accepted route to isoprenoids for several decades. Recently, an alternative pathway was discovered in algae, plant chloroplasts, and most eubacteria (*2*−*5*). The initial step in this route is the formation of 1-deoxy-D-xylulose 5-phosphoric acid (DXP) by the condensation of pyruvate and glyceraldehyde 3-phosphate in a thiamin diphosphate-dependent reaction (*6*, *7*). DXP is then converted to 2-*C*-methyl-D-erythritol 4-phosphate (MEP) by a two-step process involving rearrangement of DXP to a putative aldehyde intermediate, 2-*C*-methyl-D-erythrose 4-phosphate, followed by a NADPH-dependent reduction of the aldehyde (Figure 1). MEP is ultimately converted to both IPP and DMAPP by the action of five enzymes (*8*). Because DXP is also an intermediate in the biosynthesis of vitamin B_1 (*9*) and B_6 (*10*), MEP synthase is the first specific enzyme in the MEP pathway for isoprenoid biosynthesis.

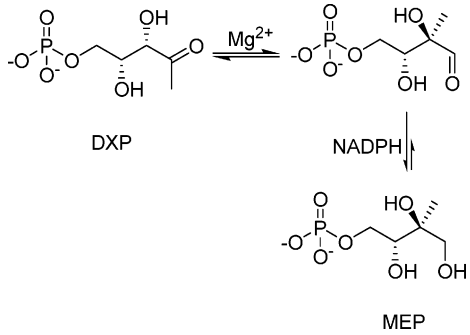

FIGURE 1: Reversible interconversion of DXP and MEP catalyzed by MEP synthase.

Several groups have studied the reactions catalyzed by MEP synthase. The stereochemistry of the rearrangement and reduction steps was reported by Proteau et al. (*11*) and Arigoni et al. (*12*). During the rearrangement, the C3−C4 carbon−carbon bond in DXP is broken and a new carbon−carbon bond formed between C2 and C4 to give the

† This work was supported by NIH Grant GM25521.

* To whom correspondence should be addressed. Telephone: (801) 581-6685. Fax: (801) 581-4391. E-mail: poulter@chem.utah.edu.

[1] Abbreviations: AHB, 2-aceto-2-hydroxybutyrate; AL, 2-acetolactate; ATP, adenosine 5′-triphosphate; BSA, bovine serum albumin; CF-DXP, 1-fluoro-1-deoxy-D-xylulose 5-phosphoric acid; CF_2-DXP, 1,1-difluoro-1-deoxy-D-xylulose 5-phosphoric acid; CF_3-DXP, 1,1,1-trifluoro-1-deoxy-D-xylulose 5-phosphoric acid; CF-ME(P), 2-*C*-fluoromethyl-D-erythritol (4-phosphate); DMAPP, dimethylallyl diphosphate; DXP, 1-deoxy-D-xylulose 5-phosphate; DXS, 1-deoxy-D-xylulose 5-phosphate synthase; Et-DXP, 1,2-dideoxy-D-hexulose 6-phosphate (Et-DXP); IPP, isopentenyl diphosphate; *i*-PrOH, isopropyl alcohol; L-Ru5P, L-ribulose-5-phosphate; MEP, 2-*C*-methyl-D-erythritol 4-phosphate; NADPH, reduced nicotinamide adenine dinucleotide phosphate; NMR, nuclear magnetic resonance; PMSF, phenylmethylsulfonyl fluoride; TBADH, *Thermoanaerobium brockii* alcohol dehydrogenase; TFA, trifluoroacetate.

10.1021/bi047312p CCC: $30.25
Published on Web 05/17/2005

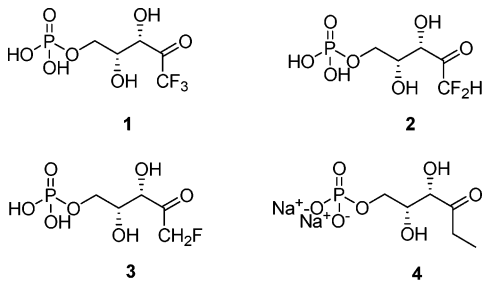

FIGURE 2: Structures of DXP analogues: (1) CF_3-DXP, (2) CF_2-DXP, (3) CF-DXP, and (4) Et-DXP.

branched-carbon skeleton in MEP. The rearrangement is followed by transfer of the *pro-S* hydrogen in NADPH to the *re* face of the transient aldehyde intermediate to generate MEP. The reduction and rearrangement steps are reversible (*13*, *14*). The addition of DXP and NADPH to *E. coli* MEP synthase is ordered with NADPH binding before DXP. Crystal structures of *E. coli* MEP synthase indicate that the active site consists of a cleft-like structure with a highly flexible loop that folds over the cleft upon substrate binding (*15*−*17*).

Two plausible mechanisms, an acid-ketol rearrangement (*18*) and a retro-aldol/aldol rearrangement (*13*), have been proposed for the conversion of DXP to MEP. Liu et al. (*19*) and we (*20*) recently reported the synthesis of a series of fluorinated analogues for DXP. A preliminary evaluation of the steady-state kinetic constants for one of those compounds, CF-DXP (*19*), suggested that the retro-aldol/aldol mechanism was operative. We now report a more extensive study, which includes the four DXP analogues shown in Figure 2.

EXPERIMENTAL PROCEDURES

Materials. All reagents were analytical-grade and were used without further purification unless noted. DXP was obtained from Echelon Biosciences, Inc. IPTG and NADPH were from USB. ATP, *Cellulomonas* sp. glycerokinase, *Cryptococcus uniguttulatus* glucose dehydrogenase, (+)-[1-^{2}H]-D-glucose, and TBADH were obtained from Sigma. γ-[^{32}P]ATP was obtained from ARC. All other chemicals were purchased from Aldrich unless otherwise noted.

General Methods. All nucleotide stock solutions were made fresh daily. NADPH solutions were made in buffer F (50 mM HEPES at pH 7.6 and 3 mM $MgCl_2$), and the concentration of the cosubstrate was calculated using ϵ_{340} = 6.22 cm^{-1} mM^{-1}. Protein concentrations were measured using the ϵ_{280} = 25 710 M^{-1} cm^{-1}/monomer as calculated from VectorNTI. Spectrophotometric assays were performed in 10 mm quartz cuvettes using an Agilent 8453 UV−vis spectrophotometer equipped with a Peltier temperature control unit. Consumption of NADPH was measured from the difference of the initial and final absorbance at 340 nm. All assays were run in duplicate. Nuclear magnetic resonance (NMR) spectra were recorded in D_2O at 500 MHz (^{1}H NMR), 125 MHz (^{13}C NMR), or 282 MHz (^{19}F NMR) using a Varian Inova 500 spectrometer. Chemical shifts were referenced to residual HOD (^{1}H NMR, 4.80 ppm), MeOH (^{13}C NMR, 49.0 ppm), and TFA (^{19}F NMR, 0.00 ppm). Mass spectrometry was performed at the University of Utah, Chemistry Department, Mass Spectrometry Facility. Silica column chromatography was performed using Silicycle silica grade 60, 230−400 mesh, and silica thin-layer chromatography (TLC) was performed on Whatman silica gel 0.25 mm aluminum plates. Silica TLC plates were visualized by a 10% solution of phosphomolybdic acid in ethanol followed by heating or by anisaldehyde stain followed by heating. The optical rotation measurement of CF-ME is reported as the specific rotation at 25 °C in g/100 mL. The syntheses of the DXP analogues were reported elsewhere (*20*).

MEP Synthase Overexpression and Purification. Cultures of *E. coli* BL21/pATK-III-46HB1 (*14*) grown in LB media at 37 °C containing 0.1 mg/mL ampicillin were induced by the addition of IPTG to a final concentration of 1 mM at an OD_{600} of 0.6. The temperature was lowered to 30 °C, and the cultures were allowed to incubate for an additional 5 h before harvesting (10 000 rpm, 25 min). A typical 500 mL culture produced ∼2.0 g of wet cell paste. Cells were sonicated on ice (6 rounds of 10 s, with a 30 s rest period) in buffer containing 50 mM NaH_2PO_4 at pH 8.0, 10 mM imidazole, 300 mM NaCl, 10 mM β-mercaptoethanol, and 1 mM PMSF. After centrifugation (10000*g*, 25 min), the supernatant was added to Ni-NTA resin (1 mL/3 mL of crude lysate) and the mixture was placed on ice under constant stirring (200 rpm) for 1 h. The suspension was then poured into a column and washed with 10 mL of buffer A (50 mM sodium phosphate at pH 8.0, 300 mM NaCl, and 20 mM imidazole) followed by stepwise elution of the protein with 2 mL each of buffers B (50 mM sodium phosphate at pH 8.0, 300 mM NaCl, and 40 mM imidazole), C (50 mM sodium phosphate at pH 8.0, 300 mM NaCl, and 100 mM imidazole), and D (50 mM sodium phosphate at pH 8.0, 300 mM NaCl, and 250 mM imidazole). Fractions containing pure protein, as judged by SDS−PAGE analysis, were combined and dialyzed against 2 × 2 L of buffer E (50 mM sodium phosphate at pH 7.6, 10 mM β-mercaptoethanol, and 20% glycerol) for 3 h each. Recombinant MEP synthase was then flash frozen and stored at −80 °C until used.

Steady-State Kinetic Analysis of DXP and CF-DXP. Assays were performed at 37 °C in a total volume of 100 μL, consisting of buffer F, 150 μM NADPH, and varying concentrations of either DXP or CF-DXP. The reactions were initiated by the addition of the enzyme. Serial dilutions of the enzyme were made into buffer F. Typically, assays contained 2 nM enzyme. Initial rates (v_i) were measured for 2−10% consumption of NADPH. Michaelis−Menten constants were calculated from data determined in duplicate at 6−7 different concentrations of the variable substrate. Kinetic data were fitted using Grafit 5.0 (Erithacus software).

Single-Turnover Kinetic Studies. Single-turnover measurements for the slow substrates (CF_2-DXP and Et-DXP) were performed under identical conditions to those for the steady-state studies for DXP and CF-DXP except for the following concentrations: 50 μM MEP synthase and 20 μM NADPH. The changes in absorbance were corrected using the three-point line drop method at 310 and 400 nm. Rate constants (k_{obs}) were calculated by fitting absorbance versus time measurements to eq 1, where y = absorbance at 340 nm, A = amplitude of the signal, t = time, and

$$y = A(1 - e^{-k_{obs}t}) + C \quad (1)$$

where C = the final absorbance. Michaelis constants were

calculated from eqs 2 and 3

$$k_{obs} = \frac{k_{max}[\text{substrate}]}{K_{1/2} + [\text{substrate}]} \quad (2)$$

$$K_{1/2} = \left(\frac{k_{-1} + k_2}{k_1}\right) \quad (3)$$

where k_{max} is the maximum rate of product formation, [substrate] is the concentration of the slow substrate analogues, and $K_{1/2}$ is the substrate analogue concentration needed to achieve one-half of k_{max}.

Single-turnover measurements for CF-DXP and DXP were performed on a KinTek SF-2001 stopped-flow apparatus. A typical reaction used 40 μL in each syringe (80 μL total). One syringe contained buffer F and DXP or CF-DXP. The other contained the buffer F, enzyme, and NADPH. The measurements were conducted at 37 °C by following the change in absorbance at 340 nm. All experiments were performed where [enzyme] > [NADPH] and at saturating levels of substrate ($\sim$10 K_m of DXP or CF-DXP). Doubling or halving the amount of enzyme had no effect on the rate. Rate constants and amplitudes were obtained by fitting the data to eq 1 to determine k_{max} using Grafit 5.0.

Primary Kinetic Isotope Effects (KIE). 4*S*-[^{2}H]NADPH was prepared by the method of Carrea et al. (*21*). The extent of deuterium incorporation was determined by ^{1}H NMR spectroscopy and was judged to be 97%. The incorporation of ^{2}H into DXP by MEP synthase was confirmed using the method of Proteau et al. (*11*). Isotope effects were determined for single turnover by the protocol described above.

Product Studies. Reactions were performed in a thick-walled NMR tube. Because of the relative instability of CF-DXP in a buffered solution ($t_{1/2} \approx 5$ h), a concentration of enzyme was chosen so that the reaction was complete within 2 h. A typical sample contained buffer F, 200 mM *i*-PrOH, 100 μM NADPH, 4 units of TBADH, 100 nM MEP synthase, 5 mM CF-DXP, and 1 mM TFA as an internal standard (0.00 ppm). All of the components except the enzyme were added to the NMR tube, and the ^{19}F resonances for CF-DXP (hydrate and ketone) were recorded. Upon the addition of the enzyme, the reaction was monitored by the appearance of a new triplet (−159.5 ppm relative to TFA) and the concomitant disappearance of the peaks for CF-DXP. Time points were taken every 5 min for the first 30 min and then every 15 min until the reaction was complete ($\sim$2 h).

Synthesis and Characterization of CF-ME. Reactions were conducted at 37 °C in 100 mM HEPES buffer at pH 7.6 containing 3 mM $MgCl_2$, 150 μM NADPH, 1 M *i*-PrOH, 10 units of TBADH, 1.0 mL CF-DXP (28 mM stock), and 1.0 mg of MEP synthase in a total volume of 5 mL. The reactions were initiated by addition of CF-DXP and followed by ^{19}F NMR spectroscopy until >98% of the CF-DXP had been consumed. Each reaction gave a single new product. After 2 h, the pH was adjusted to 8.2 and 20 units of alkaline phosphate was added, followed by incubation at room temperature for an additional hour. Protein was removed by ultrafiltration through a YM10 membrane (Millipore), and the samples were flash-frozen and lyophilized. A total of three runs were necessary to obtain sufficient material for characterization by NMR spectroscopy. The combined solids were resuspended in $CHCl_3$/MeOH (90:10) and applied to silica gel. Elution with $CHCl_3$/MeOH (80:20, R_f = 0.27) followed by rotory evaporation to remove the solvent gave a colorless oil. ^{1}H NMR (ppm, D_2O) δ: 3.64−3.73 (m, 3H), 3.82−3.89 (m, 2H), 4.57 (AB quartet, 2H, J = 46.7, 7.7 Hz). ^{13}C NMR (ppm, D_2O) δ: 61.6 (d, J = 6.0 Hz), 61.8 (d, J = 2.5 Hz), 72.6 (d, J = 3.5 Hz), 75.4 (d, J = 16.5 Hz), 83.5 (d, J = 170 Hz). ^{19}F NMR (ppm, D_2O) δ: −159.4 (t, J = 46.7 Hz). $[\alpha]^{25}_D$ +2.5 (*c* 0.2, H_2O). HRMS (CI, M + H) *m*/*z*: calcd for $C_5H_{12}FO_4$, 155.0714; found, 155.0710.

Assay for Aldolase Activity. Glycoaldehyde 2-phosphate (G2P) was prepared from 3.1 mmol of α-glycerol 3-phosphate (Sigma) and 6.2 mmol of $NaIO_4$ in 15 mL of H_2O. The pH of the solution was adjusted to 6.0 and allowed to stir for 5 h. The reaction was quenched with 3.5 mmol of glycerol, which consumed unreacted periodate. The precipitate was removed by filtration, and the aqueous solution was lyophilized. The solid was dissolved in *i*-PrOH/H_2O (75:25) and chromatographed over cellulose. Fractions containing G2P were collected, lyophilized, and stored at −20 °C. The ^{1}H NMR spectrum of G2P agreed with a spectrum reported for G2P synthesized by an alternative method (*22*).

[^{32}P]G2P was prepared as follows. To a total reaction volume of 1 mL of buffer containing 50 mM CHES and 3 mM $MgCl_2$ at pH 7.5 was added 125 μCi [γ-^{32}P]ATP (6000 Ci/mmol), 10 mM glycerol, and 10 units of glycerokinase. After 2 h at room temperature, a 5-fold excess of $NaIO_4$ (10.7 mg, 50 mM final) was added and the mixture was incubated at room temperature for 3 h, at which time 100 mM ethylene glycol was added to destroy excess periodate. Cold acetone (1 mL) was added, and the mixture was stored at −20 °C overnight. The precipitate was removed by filtration, and the aqueous solution was lyophilized. The solid was dissolved in *i*-PrOH/H_2O (70:30) and chromatographed over cellulose. Fractions containing a single radioactive spot with the same R_f as cold G2P were pooled and concentrated under vacuum.

Incubations to detect aldolase activity for hydroxyacetone and G2P were carried out in 50 mM HEPES buffer at pH 7.6 containing 2 μM MEP synthase, 3 mM $MgCl_2$, 300 μM NADPH, 5 mM cold G2P, $\sim$0.1 nCi [^{32}P]G2P, and varying concentrations of hydroxyacetone in a total reaction volume of 50 μL. At 4 h intervals, 4−6 μL portions of the mixture were spotted on cellulose TLC plates. The plates were developed in 68:32 THF/H_2O [0.1% (v/v) TFA] and exposed by phosphorimaging (Molecular Dynamics).

RESULTS

Steady-State Kinetic Studies for DXP and CF-DXP. Initial velocities (v_i) for recombinant *E. coli* MEP synthase were measured at 340 nm by monitoring oxidation of NADPH. Apparent Michaelis constants for DXP and CF-DXP at a saturating concentration of NADPH were determined from plots of specific activity [μmol min^{-1} (mg enzyme)$^{-1}$] versus substrate concentration (Figure 3). The values are listed in Table 1.

Conversion of CF-DXP to CF-MEP. The conversion of CF-DXP to CF-MEP (see Scheme 1) was followed by ^{19}F NMR spectroscopy (see Figure 4A). A nucleotide cofactor

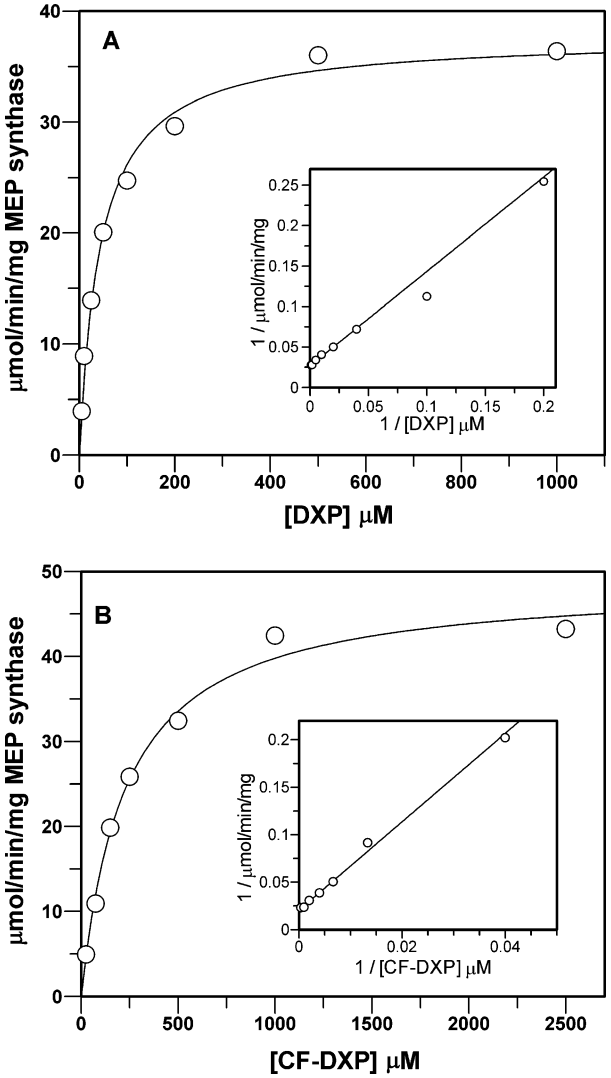

FIGURE 3: Rate versus substrate concentration for (A) DXP and (B) CF-DXP, respectively, at 150 μM NADPH.

Table 1: Steady-State Kinetic Constants for MEP Synthase in the Presence of CF-DXP or DXP

substrate	k_{cat} (s^{-1})	K_m (μM)	k_{cat}/K_m (s^{-1} M^{-1}) × 10^5
CF-DXP[a]	37 ± 2	227 ± 25	1.62 ± 0.02
DXP	29 ± 1	45 ± 4	6.44 ± 0.07
NADPH[b]		0.5 ± 0.2	

[a] $K_m^{NADPH} = 0.5 \pm 0.1$ at saturating [CF-DXP]. [b] At saturating [DXP] (ref *14*). $K_D^{NADPH} = 0.45 \pm 0.15$ at saturating [DXP] (ref *19*).

regeneration system (*23*) was used to prevent inhibition by $NADP^+$ as the reaction proceeded. At $t = 0$, the spectrum for CF-DXP showed well-resolved resonances for the fluoromethyl groups in the ketone (−158.6 ppm) and hydrate (−157.2 ppm) of CF-DXP. Upon addition of MEP synthase, the resonances for the ketone and hydrate decreased over 2 h with the concomitant appearance of a new triplet at −159.2 ppm for the fluoromethyl group in CF-MEP. The amount of CF-MEP produced was determined by dividing the intensity of the new resonance by the sum of the intensities of all three. A time course for the reaction is shown in Figure 4B. The ^{19}F NMR spectrum indicated that CF-MEP is the only product. In addition, the 77:23 ratio of CF-DXP and the corresponding hydrate remained constant as the reaction proceeded to completion. Thus, the equilibrium between CF-

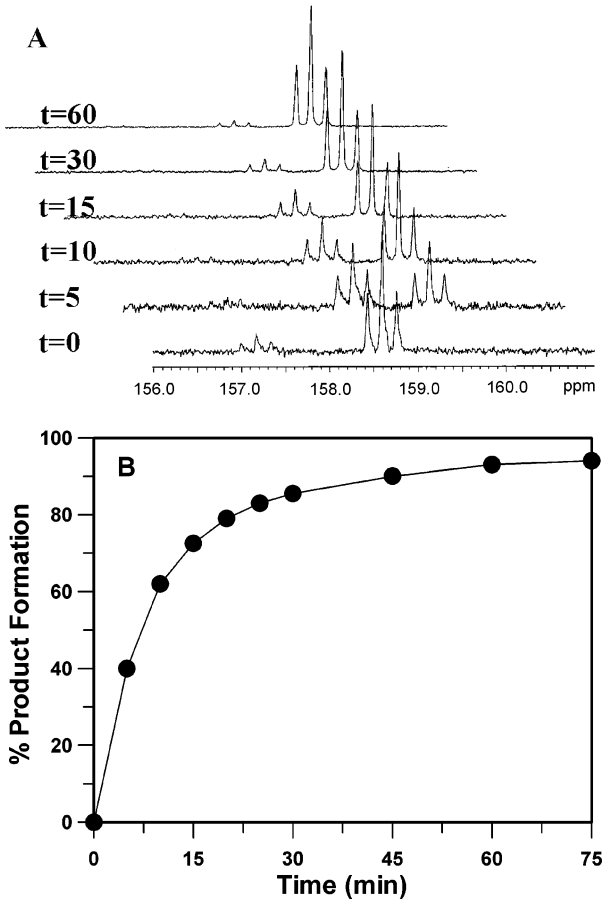

FIGURE 4: (A) Stacked plot of ^{19}F NMR spectra taken during incubation of a sample containing 5 mM CF-DXP, 0.10 mM NADPH, and 100 nM MEP synthase as described in the Experimental Procedures. Chemical shifts were referenced to sodium trifluoroacetate (0.0 ppm, internal standard). ^{19}F resonances were seen for the fluoromethyl moieties in CF-DXP (ketone, −158.6 ppm), CF-DXP (hydrate, −157.2 ppm), and CF-MEP (−159.2 ppm). The reaction was >98% complete after 2 h. (B) Plot of product formation versus time. The percentage of CF-MEP was determined by integration of the intensities of the peaks for the ketone, hydrate, and product.

Scheme 1: Conversion of CF-DXP to CF-MEP

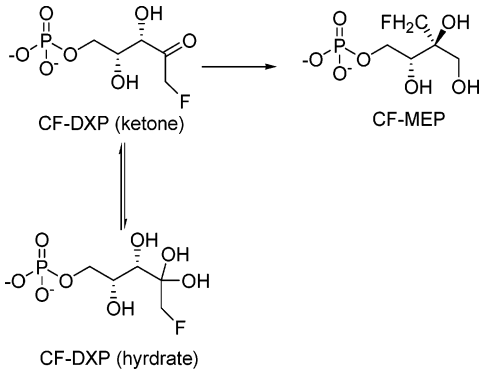

DXP and the hydrate appears to be established more rapidly than the conversion of CF-DXP to CF-MEP.

Characterization of CF-ME. Figure 4A shows the appearance of a new triplet following the addition of MEP synthase to the reaction mixture. A large scale reaction with CF-DXP (~2 mg) and MEP synthase, using the NADPH regeneration system, gave enough material for analysis by NMR spectroscopy and MS. The product was hydrolyzed with alkaline

phosphatase to provide the corresponding alcohol. After lyophilization, the tetrol was extracted into chloroform/methanol and purified over silica gel. The exact mass of the new product by chemical ionization corresponded to the calculated value for CF-ME. A ^{19}F NMR spectrum of CF-ME has a triplet at −159.4 ppm (J = 46.7 Hz) characteristic of a fluoromethyl moiety. The fluoromethyl group also gave a well-resolved AB quartet at 4.57 ppm (J = 46.7 Hz) in the ^{1}H NMR spectrum. Integration of the entire ^{1}H NMR spectrum reveals that seven hydrogens are directly attached to the carbon framework, as expected for CF-ME. The ^{13}C NMR spectrum also shows the appearance of five resonances, corresponding to the carbon framework of CF-ME (NMR spectra for CF-ME can be found in the Supporting Information). In addition, the specific rotation of CF-ME ($[\alpha]^{25}_{D}$ +2.5) has the same sign as ME ($[\alpha]^{25}_{D}$ +7.0) (*24*).

Single-Turnover and Stopped-Flow Studies. Turnover was not observed for CF_2-DXP, CF_3-DXP, and Et-DXP under normal assay conditions. Single-turnover conditions were used with an excess of enzyme, a fixed saturating concentration of NADPH, and varying concentrations of the DXP analogues. Under these conditions, all of the DXP analogues except CF_3-DXP were alternate substrates. First-order rate constants were calculated by fitting the data to eq 1 (data not shown). Michaelis constants were determined from the plots of k_{obs} versus substrate concentration for CF_2-DXP (Figure 5A) and Et-DXP (Figure 5B) at 20 μM NADPH (Table 2).

Stopped-flow measurements were used to obtain first-order rate constants for CF-DXP and DXP under single-turnover conditions. MEP synthase was used in excess of a fixed saturating concentration of NADPH. CF-DXP and DXP concentrations were ~10 K_m as determined under steady-state conditions. NADPH, the first substrate to add in the ordered binding mechanism (*14*), was preincubated with the enzyme to avoid hysteresis. Each transient showed single-exponential kinetics (see Figure 6) and was fitted to eq 1. The values of k_{max} for CF-DXP and DXP were identical (61 s^{-1}) and were in good agreement with the values of k_{cat} obtained under steady-state conditions for both CF-DXP (37 s^{-1}) and DXP (29 s^{-1}).

Multiple-turnover experiments were performed with excess NADPH to determine if burst kinetics were observed upon rapid mixing of the enzyme−NADPH binary complex with saturating levels of CF-DXP or DXP (data not shown). No burst of $NADP^+$ formation was detected for either substrate, and the linear steady-state rate of NADPH oxidation was in agreement with the value for k_{cat} obtained under steady-state conditions.

The values of $K_{1/2}$ for CF_2-DXP and Et-DXP obtained from single-turnover experiments were 2.1 and 1.5 mM, respectively; whereas, the values of K_m for CF-DXP and DXP derived from steady-state conditions were 0.23 and 0.05 mM, respectively (see Table 2). Collectively, these results suggest that product release is not rate-limiting and that the enzyme does not tolerate a significant increase in steric bulk at C1 of DXP.

Kinetic Isotope Effects Using 4S-[^{2}H]NADPH with DXP and CF-DXP. MEP synthase catalyzes two reactions, the rearrangement of DXP to an aldehyde and reduction of the aldehyde to MEP. The assay for the enzyme measures the rate of the second step. Previous efforts to trap the aldehyde have not been successful (*13*, *14*), and in all probability, the aldehyde is not released from the enzyme during turnover. Because the electron-withdrawing effect of fluorine at C1 of DXP is expected to exert its influence on the first step, it is important to determine if rearrangement or hydride transfer is rate-limiting. For this purpose, single-turnover rates were measured for 4*S*-[^{2}H]NADPH to see if a primary deuterium

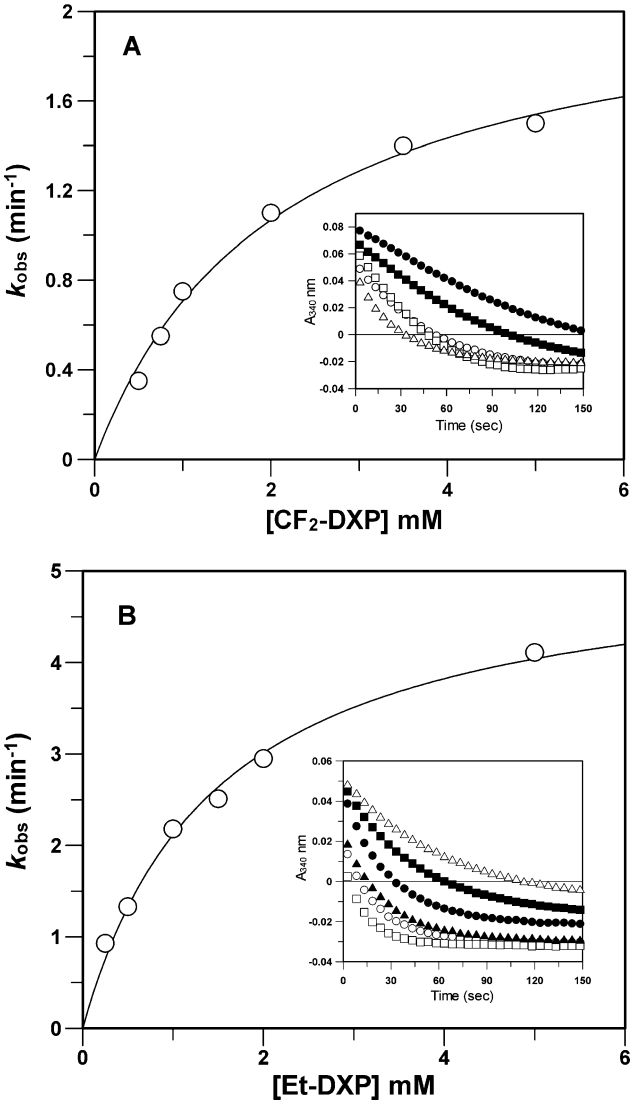

FIGURE 5: Plots of k_{obs} versus [CF_2-DXP] (A) and [Et-DXP] (B) at 37 °C for [NADPH] = 20 μM and [MEP synthase] = 50 μM. (Inset) Representative single-exponential traces for CF_2-DXP and Et-DXP.

Table 2: Kinetic Constants for DXP and the Related Analogues[a]

substrate	k_{max}[b] (min^{-1})	K[c] (mM)	k_{max}/K (min^{-1} mM^{-1})	k_{rel}/K[d]
CF_3-DXP	ND[e]	ND	ND	ND
CF_2-DXP	2.2 ± 0.1	2.1 ± 0.3	1.1	1.4×10^{-5}
CF-DXP	3647 ± 17	0.23 ± 0.03	1.6×10^4	0.22
Et-DXP	5.3 ± 0.2	1.5 ± 0.1	3.5	4.8×10^{-5}
DXP	3669 ± 37	0.05 ± 0.01	7.3×10^4	1.0

[a] At pH 7.6 and 37 °C. [b] For the slow substrates (CF_2-DXP and Et-DXP), k_{max} was determined from parts A and B of Figure 5. For the fast substrates (CF-DXP and DXP), a k_{max} value was determined from parts A and B of Figure 6. [c] For the slow substrates, a $K_{1/2}$ value was derived from a plot of k_{obs} versus [analogue]. The K_m values for CF-DXP and DXP are from Table 1. [d] $^{\text{analogues}}(k_{rel}/K)/^{\text{DXP}}(k_{max}/K)$. [e] No activity was detected.

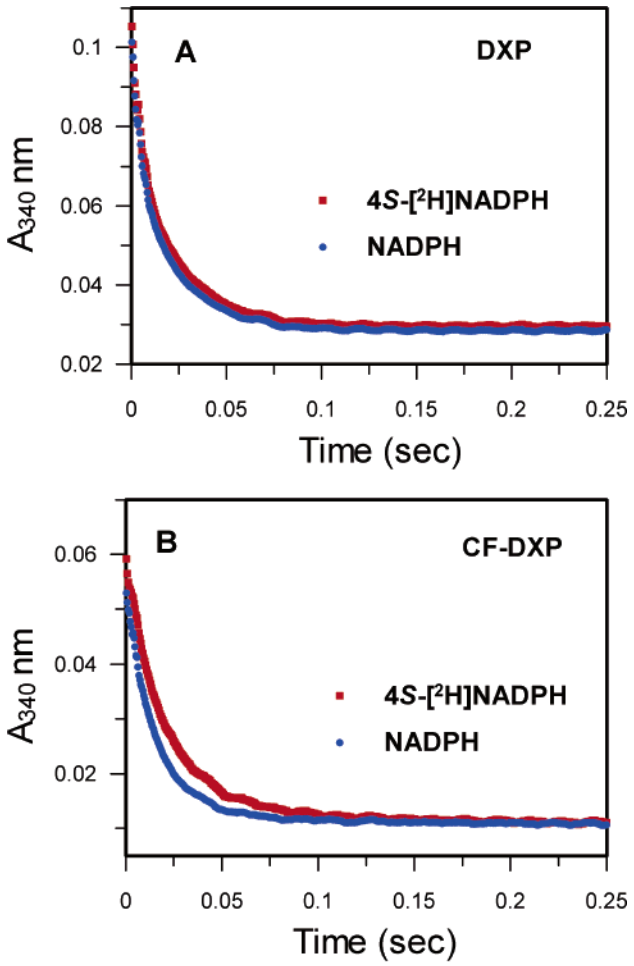

FIGURE 6: Deuterium kinetic isotope effects observed for DXP (A) and CF-DXP (B) with (red square) 4*S*-[^{2}H]NADPH or (blue circle) NADPH. (A) Plot of A_{340} versus time for DXP. Reactions were initiated by combining 40 μL of 150 μM MEP synthase, 40 μM NADPH or 4*S*-[^{2}H]NADPH, 50 mM HEPES at pH 7.6, 3 mM $MgCl_2$ with 40 μL of 1 mM DXP, 50 mM HEPES at pH 7.6, and 3 mM $MgCl_2$. (B) Plot of A_{340} versus time for CF-DXP. The conditions were the same as described for A with the following exceptions: DXP was replaced with 5.0 mM CF-DXP, and the concentration of NADPH and 4*S*-[^{2}H]NADPH was 30 μM. The curves are an average of 6−8 runs. Note: the path length of the observation chamber was 0.5 cm. The amplitudes of the signals obtained from fits to eq 1 were 0.041 (NADPH) and 0.045 (4*S*-[^{2}H]NADPH) for CF-DXP and 0.066 (NADPH and 4*S*-[^{2}H]-NADPH) for DXP, respectively.

Table 3: Deuterium Isotope Effects for Reduction of CF-DXP and DXP by 4*S*-[^{2}H]NADPH[a]

	$^{H}k_{max}$[b]	$^{D}k_{max}$	$^{H}k/^{D}k$
DXP	3669 ± 37	3587 ± 42	1.02 ± 0.02
CF-DXP	3647 ± 17	2728 ± 21	1.34 ± 0.01

[a] At pH 7.6 and 37 °C. [b] Values taken from Table 2.

isotope effect was seen for DXP and CF-DXP. As shown in Figure 6A, no isotope effect was observed when DXP was converted to MEP using 4*S*-[^{2}H]NADPH. In contrast, a small primary kinetic isotope effect was observed for CF-DXP (Figure 6B). The results are listed in Table 3.

Tests for Aldolase Activity. We attempted to detect aldolase activity for MEP synthase by incubation of the enzyme with hydroxyacetone (50 mM) and glycoaldehyde 2-phosphate (G2P, 5 mM) in the presence of NADPH. The reaction was monitored by the changes in absorbance at 340 nm as the nucleotide cofactor was being oxidized. However, a high background was observed when G2P or hydroxyacetone were incubated with NADPH in the absence of the enzyme.

A more sensitive assay for aldolase activity was attempted using [^{32}P]G2P. The radioactive precursor was prepared in a single pot chemoenzymatically to minimize handling and exposure. Incubation of MEP synthase with the aldol substrates and NADPH, followed by thin-layer chromatography under conditions that resolved the substrates from MEP and DXP and autoradiography, showed no spots for formation of ^{32}P-labeled DXP or MEP.

DISCUSSION

MEP synthase catalyzes two reactions, the rearrangement of the linear carbon skeleton in DXP to the branched skeleton in MEP and the subsequent reduction of the putative aldehyde formed during the rearrangement (see Figure 1). Under normal conditions, the addition of substrates is ordered with NADPH binding before DXP (*14*) and the aldehyde intermediate is not released from the active site. There is precedent for the type of carbon skeletal rearrangement catalyzed by MEP synthase. 3,4-Dihydroxy-2-butanone 4-phosphate synthase converts L-ribulose 5-phosphate (L-Ru5P) to 3,4-dihydroxy-2-butanone 4-phosphate during riboflavin biosynthesis (*25*). Ketol-acid reductoisomerase catalyzes the conversion of either (2*S*)-acetolactate (AL) or (2*S*)-2-aceto-2-hydroxybutyrate (AHB) to (2*R*)-2,3-dihydroxy-3-isovalerate or (2*R*,3*R*)-2,3-dihydroxy-3-methylvalerate, respectively (*26*). Finally, L-ribulose-5-phosphate 4-epimerase catalyzes the interconversion of L-Ru5P and D-xylulose-5-phosphate (D-Xu5P) (*27*). The rearrangement catalyzed by 3,4-dihydroxy-2-butanone 4-phosphate synthase and ketol-acid reductoisomerase involves either protonation or coordination of divalent metal to the carbonyl moiety in the substrate, followed by rearrangement to the electron-deficient carbonyl carbon (*25*, *26*). The retro-aldol/aldol rearrangement catalyzed by Ru5P epimerase gives the rearranged aldol product, but the enzyme does not catalyze its subsequent reduction. Although the X-ray crystal structures of MEP synthase, ketol-acid reductoisomerase, and Ru5P epimerase show highly conserved acidic residues in the active-site pocket and a deep active-site cleft that excludes the bulk solvent (*15*, *28*, *29*), there is no obvious similarity among the proteins that might provide a clue about the mechanism of the rearrangement of DXP to MEP (see Scheme 2). Recently, Tanner et al. (*30*) and Cleland et al. (*31*, *32*) reported very low levels of aldolase activity (~0.003%) when Ru5P epimerase was incubated with dihydroxyacetone and G2P. In a related experiment, we incubated [^{32}P]G2P, hydroxyacetone, and NADPH with MEP synthase but were unsuccessful in an effort to detect aldolase activity for MEP synthase.

Fluorine analogues CF-DXP, CF_2-DXP, and CF_3-DXP were designed to probe for the development of charge in the transition state of the rearrangement step. The α-ketol rearrangement requires either protonation or coordination of divalent metal of the ketone to facilitate carbon−carbon bond cleavage. Prior studies have demonstrated that substitution of hydrogen by fluorine at the β position reduces the basicity of ketones by ~2−3 p*K* units per fluorine substitution (*33*).

Scheme 2: Two Possible Mechanisms Catalyzed by MEP Synthase: (a) α-Ketol Rearrangement, (b) Retro-aldol/Aldol Rearrangement (X = H^+ or Divalent Metal)

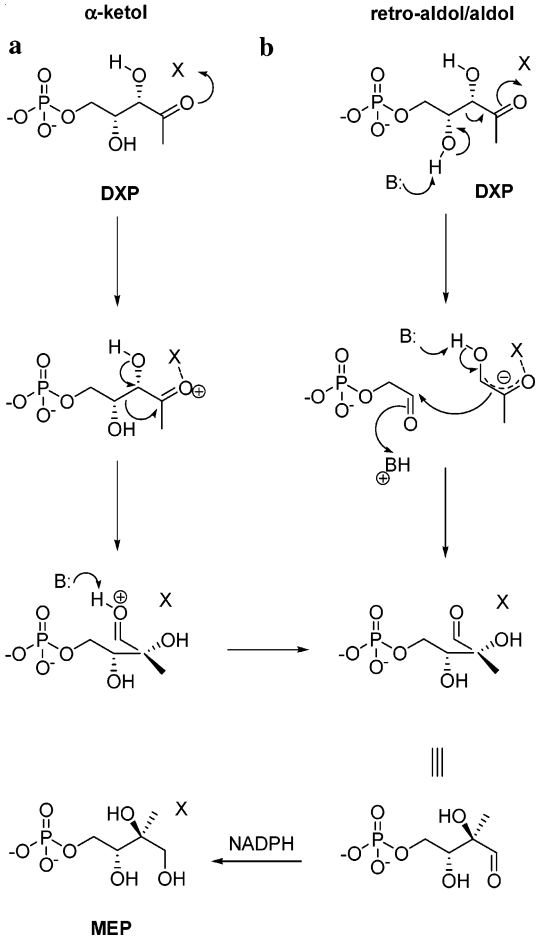

Therefore, one would expect that protonation or complexation of divalent metal to the corresponding ketone would become less favored with increasing fluorine substitution. Typically, the barrier for rearrangements are low and formation of the carbenium ion undergoing rearrangement is rate-limiting. While the fluorine might accelerate the rearrangement step, it would retard formation of the oxocarbenium ion. In contrast, if the retro-aldol/aldol mechanism were operative, carbon−carbon bond cleavage might be facilitated because the developing enolate in the retro-aldol step should be stabilized by fluorine substitution at the β position of DXP. When the chemical steps are rate-limiting, the fluorines should decrease the rate of the acid-ketol rearrangement and perhaps accelerate the retro-aldol mechanism.

In addition to destabilizing protonation of the ketone moiety in DXP, fluorine substitution at the β position shifted the ketone/ketone hydrate equilibrium toward hydration. The percentage of ketone hydrate increased with increasing fluorine substitution in the order CF-DXP (23% hydrate), CF_2-DXP (98% hydrate), and CF_3-DXP (>99.9% hydrate). The di- and trifluorinated analogues were modest inhibitors of MEP synthase with IC_{50} values in the millimolar range. Poor binding could reflect the greater proportion of hydrate in the equilibrium mixture or the increased steric bulk at C1 resulting from replacing the hydrogens with fluorine. While we were not able to probe the effect of hydration on the binding of the DXP analogues, it is clear that binding to MEP synthase is sensitive to substitutions that increase the steric bulk of the methyl group in DXP. Et-DXP was not turned over at a measurable rate under normal catalytic conditions, and the IC_{50} that we measured for the ethyl analogue was slightly higher than those for CF_3-DXP and CF_2-DXP (*20*). Proteau et al. also reported that Et-DXP was not a substrate for the *Synechocystis* sp. enzyme but was instead a competitive inhibitor against DXP with K_i^{Et-DXP} ~4-fold larger than K_m^{DXP}.

We, also, did not observe turnover for CF_2-DXP, CF_3-DXP, and Et-DXP under normal catalytic conditions. However, at high enzyme concentrations under single-turnover conditions, all of the analogues, except for CF_3-DXP, were alternate substrates. Et-DXP and CF_2-DXP were turned over approximately 700 and 1700 times slower, respectively, than CF-DXP and DXP. The substantially slower rate observed for CF_2-DXP could result from deactivation of the carbonyl group toward protonation, a rate-limiting conversion of the hydrate to the ketone, or crowding in the active site that misaligns the molecule. Of these possibilities, we favor the latter explanation. For example, the single fluorine in CF-DXP did not result in a decrease in the rate for its conversion to CF-MEP. In addition, the rate of dehydration of the CF-DXP hydrate was substantially faster than the enzyme-catalyzed rearrangement of CF-DXP to CF-MEP during the preparative scale reaction. However, Et-DXP, which is not hydrated and has no β fluorines, is also a poor substrate. The major factor in the large decrease in k_{max}/K for both CF_2-DXP and Et-DXP relative to DXP results from k_{max}, presumably because the molecule is not properly aligned in the active site, although an electronic effect from fluorine substitution is possible.

Of the analogues that we examined, CF-DXP gave the most revealing information about the mechanism of the rearrangement step. The values of k_{cat} for DXP and CF-DXP were virtually identical, and K_m^{CF-DXP} was only ~5 K_m^{DXP}. These observations are consistent with a retro-aldol/aldol mechanism for the rearrangement step. A similar mechanism was recently proposed by Liu et al., who reported $k_{cat}^{CF-DXP} = 4.5\ s^{-1}$ and $k_{cat}^{DXP} = 21.3\ s^{-1}$ from steady-state measurements for the *E. coli* enzyme (*19*).

However, this evidence in support of a retro-aldol/aldol mechanism rests on the assumption that rearrangement is at least partially rate-limiting during the rearrangement/reduction of CF-DXP. If reduction were rate-limiting, a primary kinetic isotope effect should be seen during a single-turnover experiment when 4*S*-[^{2}H]NADPH was the cosubstrate. Because we did not see a burst for NADPH oxidation during our multiple-turnover experiments, we conclude it is unlikely that product release is rate-limiting. We also did not observe an isotope effect on k_{max} when MEP synthase was incubated with DXP and 4*S*-[^{2}H]NADPH in the single-turnover experiment, suggesting that a step prior to hydride transfer, presumably rearrangement, was rate-limiting. In contrast, a similar experiment with CF-DXP gave a small but reproducible primary isotope effect ($^D k_{max} = 1.34$). This finding was particularly interesting because it indicates that hydride transfer has now become partially rate-limiting. Thus, the rate of the rearrangement step appears to be accelerated for CF-DXP relative to the normal substrate. We cannot determine the magnitude of the rate enhancement from our studies, although it is probably small. If hydride transfer were

completely rate-limiting, a primary isotope effect of $^{D}k_{max} \sim 7-10$ would be expected assuming a "symmetrical" transition state and no contributions from tunneling (*34*). The observed isotope effect was only 3−5% of the "classical" maximal value and could be accounted for by a relatively small increase in k_{max} for CF-DXP relative to DXP. In conjunction with the studies reported by Liu and co-workers (*19*), the effect of fluorine substitution in DXP is consistent with a retro-aldol/aldol mechanism but would not be expected for an acid-catalyzed α-ketol rearrangement.

Recent steady-state kinetic isotope effect studies with 4*S*-[^{2}H]NADPH, 4*S*-[^{2}H]NADH, and DXP and MEP synthase from *Mycobacterium tuberculosis* enzyme suggested that NADPH was "sticky" and that release of at least one of the products or an enzyme conformational change(s) was partially rate-limiting with NADPH (*35*). In addition, the *M. tuberculosis* enzyme was proposed to utilize a random mechanism for substrate binding, although a preferred order of substrate addition, where NADPH precedes DXP, was not ruled out.

Similar steady-state isotope experiments were not conducted with the *E. coli* enzyme, and we cannot rule out the possibility that substrate binding and release is slow relative to chemistry. However, NADPH was preincubated with MEP synthase during our single-turnover experiments based on previous reports that the *E. coli* enzyme obeys a strictly ordered mechanism with NADPH binding prior to DXP (*14*), thus making the NADPH-binding step invisible. Therefore, the observed rates (k_{max}) include enzyme conformational change(s), rearrangement, and reduction. While we did not directly probe enzyme conformational change(s) as a rate-limiting step, it is difficult to see how the substitution of a single fluorine at the C1 position of DXP would significantly alter this rate. Therefore, the isotope effect observed in the presence of CF-DXP and 4*S*-[^{2}H]NADPH most likely reflects changes in the rate of the rearrangement and/or the reduction step(s).

In conclusion, MEP synthase catalyzes a rate-limiting rearrangement of DXP to an aldehyde intermediate, followed by an NADPH-dependent reduction of the aldehyde to MEP. When one of the C1 hydrogens of DXP was replaced by fluorine, k_{max} for the overall reaction obtained during single-turnover studies did not change. Kinetic isotope studies with 4*S*-[^{2}H]NADPH indicated that rearrangement was rate-limiting with DXP, while reduction was partially rate-limiting for CF-DXP. These observations are consistent with a retro-aldol/aldol mechanism for the reaction.

ACKNOWLEDGMENT

We thank Prof. Janet Lindsey for the use of the stopped-flow instrument.

SUPPORTING INFORMATION AVAILABLE

^{1}H, ^{13}C, and ^{19}F NMR spectra of CF-ME. This material is available free of charge via the Internet at http://pubs.acs.org.

REFERENCES

1. Sacchettini, J. C., and Poulter, C. D. (1997) Biochemistry: Creating isoprenoid diversity, *Science 277*, 1788−1789.
2. Flesch, G., and Rohmer, M. (1988) Prokaryotic hopanoids: The biosynthesis of the bacteriohopane skeleton, *Eur. J. Biochem. 175*, 405−411.
3. Rohmer, M., Sutter, B., and Sahm, H. (1989) Bacterial sterol surrogates. Biosynthesis of the side-chain of bacteriohopanetetrol and of a carbocyclic pseudopentose from ^{13}C-labelled glucose in *Zymomonas mobilis*, *J. Chem. Soc., Chem. Commun.*, 1471−1472.
4. Rohmer, M., Knani, M., Simonin, P., Sutter, B., and Sahm, H. (1993) Isoprenoid biosynthesis in bacteria: A novel pathway for the early steps leading to isopentenyl diphosphate, *Biochem. J. 295*, 517−524.
5. Putra, S. R., Disch, A., Bravo, J.-M., and Rohmer, M. (1998) Distribrution of mevalonate and glyceraldehyde 3-phosphate/pyruvate routes for isoprenoid biosynthesis in some Gram-negative bacteria and mycobacteria, *FEMS Microbiol. Lett. 164*, 169−175.
6. Sprenger, G. A., Schorken, U., Wiegert, T., Grolle, S., deGraaf, A. A., Taylor, S. V., Begley, T. P., Bringer-Meyer, S., and Sahm, H. (1997) Identification of a thiamin-dependent synthase in *Escherichia coli* required for the formation of the 1-deoxy-D-xylulose 5-phosphate precursor to isoprenoids, thiamin, and pyridoxol, *Proc. Natl. Acad. Sci. U.S.A. 94*, 12857−12862.
7. Lois, L. M., Campos, N., Putra, S. R., Danielson, K., Rohmer, M., and Boronat, A. (1998) Cloning and characterization of a gene from *Escherichia coli* encoding a transketolase-like enzyme that catalyzes the synthesis of D-1-deoxyxylulose 5-phosphate, a common precursor for isoprenoid, thiamin, and pyridoxol biosynthesis, *Proc. Natl. Acad. Sci. U.S.A. 95*, 2105−2110.
8. Seto, H., and Kuzuyama, T. (2003) Diversity of the biosynthesis of the isoprene units, *Nat. Prod. Rep. 20*, 171−183.
9. Backstrom, A. D., Austin, R., McMordie, A. S., and Begley, T. P. (1995) Biosynthesis of thiamin I: The function of the thiE gene product, *J. Am. Chem. Soc. 117*, 2351−2352.
10. Kennedy, I. A., Hill, R. E., Pauloski, R. M., Sayer, B. G., and Spenser, I. D. (1995) Biosynthesis of vitamin B6: Origin of pyridoxine by the union of two acyclic precursors, 1-deoxy-D-xylulose and 4-hydroxy-L-threonine, *J. Am. Chem. Soc. 117*, 1661−1662.
11. Proteau, P. J., Woo, Y.-H., Williamson, T., and Phaosiri, C. (1999) Stereochemistry of the reduction step mediated by recombinant 1-deoxy-D-xylulose 5-phosphate isomeroreductase, *Org. Lett. 1*, 921−923.
12. Arigoni, D., Giner, J.-L., Sagner, S., Wungsintaweekul, J., Zenk, M. H., Kis, K., Bacher, A., and Eisenreich, W. (1999) Stereochemical course of the reduction step in the formation of 2-*C*-methylerythritol from the terpene precursor 1-deoxyxylulose in higher plants, *Chem. Commun.*, 1127−1128.
13. Hoeffler, J.-F., Tritsch, D., Grosdemange-Billiard, C., and Rohmer, M. (2002) Isoprenoid biosynthesis via the methylerythritol phosphate pathway. Mechanistic investigations of the 1-deoxy-D-xylulose 5-phosphate reductoisomerase, *Eur. J. Biochem. 269*, 4446−4457.
14. Koppisch, A. T., Fox, D. T., Blagg, S. J. B., and Poulter, C. D. (2002) *E. coli* MEP synthase: Steady-state kinetic analysis and substrate binding, *Biochemistry 41*, 236−243.
15. Reuter, K., Sanderbrand, S., Jomaa, H., Wiesner, J., Steinbrecher, I., Beck, E., Hintz, M., Klebe, G., and Stubbs, M. (2002) Crystal structure of 1-deoxy-D-xylulose-5-phosphate reductoisomerase, a crucial enzyme in the non-mevalonate pathway of isoprenoid biosynthesis, *J. Biol. Chem. 277*, 5378−5384.
16. Steinbacher, S., Kaiser, J., Eisenreich, W., Huber, R., Bacher, A., and Rohdich, F. (2003) Structural basis of fosmidomycin action revealed by the complex with 2-*C*-methyl-D-erythritol 4-phosphate synthase (Isp C), *J. Biol. Chem. 278*, 18401−18407.
17. Sweeney, A. M., Lange, R., Fernandes, R. P. M., Schulz, H., Dale, G. E., Douangamath, A., Proteau, P. J., and Oefner, C. (2005) The crystal structure of *E. coli* 1-deoxy-D-xylulose-5-phosphate reductoisomerase in a ternary complex with the antimalarial compound fosmidomycin and NADPH reveals a tight-binding closed enzyme conformation.
18. Kuzuyama, T., Takahashi, S., Watanabe, W., and Seto, H. (1998) Direct formation of 2-*C*-methyl-D-erythritol 4-phosphate from 1-deoxy-D-xylulose 5-phosphate by 1-deoxy-D-xylulose 5-phosphate reductoisomerase, a new enzyme in the non-mevalonate pathway to isopentenyl diphosphate, *Tetrahedron Lett. 39*, 4509−4512.
19. Wong, A., Munos, J. W., Devasthali, V., Johnson, K. A., and Liu, H.-w. (2004) Study of 1-deoxy-D-xylulose-5-phosphate reductoisomerase: Synthesis and evaluation of fluorinated substrate analogues, *Org. Lett. 6*, 3625−3628.
20. Fox, D. T., and Poulter, C. D. (2005) Synthesis and evaluation of 1-deoxy-D-xylulose 5-phosphoric acid analogues as alternate

substrates for methylerythritol phosphate synthase, *J. Org. Chem. 70*, 1978−1985.
21. Ottolina, G., Riva, S., Carrea, G., Danieli, B., and Buckmann, A. F. (1989) Enzymatic synthesis of [4*R*-^{2}H]NAD(P)H and [4*S*-^{2}H]-NAD(P)H and determination of the stereospecificity of 7α- and 12α-hydroxysteroid dehydrogenase, *Biochim. Biophys. Acta 998*, 173−178.
22. Pitsch, S., Pombo-Villar, E., and Eschenmoser, A. (1994) Chemistry of α-aminonitriles. Part 13. Formation of 2-oxoethyl phosphates ("glycoaldehyde phosphates") from *rac*-oxiranecarbonitrile and inorganic phosphate and on (formal) constitutional relationships between 2-oxoethyl phosphates and oligo(hexo- and pentopyranosyl)nucleotide backbones, *Helv. Chim. Acta 77*, 2251−2285.
23. Keinan, E., Hafeli, E. K., Seth, K. K., and Lamed, R. (1986) Thermostable enzymes in organic synthesis. 2. Asymmetric reduction of ketones with alcohol dehydrogenase from *Thermoanaerobium brockii*, *J. Am. Chem. Soc. 108*, 162−169.
24. Duvold, T., Cali, P., Bravo, J.-M., and Rohmer, M. (1997) Incorporation of 2-*C*-methyl-D-erythritol, a putative isoprenoid precursor in the mevalonate-independent pathway, into ubiquinone and menaquinone of *Escherichia coli*, *Tetrahedron Lett. 38*, 6181−6184.
25. Steinbacher, S., Schiffmann, S., Richter, G., Huber, R., Bacher, A., and Fischer, M. (2003) Structure of 3,4-dihydroxy-2-butanone 4-phosphate synthase from *Methanococcus jannaschii* in complex with divalent metal ions and the substrate ribulose 5-phosphate, *J. Biol. Chem. 278*, 42256−42265.
26. Dumas, R., Biou, V., Halgand, F., Douce, R., and Duggleby, R. G. (2001) Enzymology, structure, and dynamics of acetohydroxy acid isomeroreductase, *Acc. Chem. Res. 34*, 399−408.
27. Johnson, A. E., and Tanner, M. E. (1998) Epimerization via carbon−carbon bond cleavage. L-Ribulose-5-phosphate 4-epimerase as a masked class II aldolase, *Biochemistry 37*, 5746−5754.
28. Luo, Y., Samuel, J., Mosimann, S. C., Lee, J. E., Tanner, M. E., and Strynadka, N. C. J. (2001) The structure of L-ribulose-5-phosphate 4-epimerase: An aldolase-like platform for epimerization, *Biochemistry 40*, 14763−14771.
29. Biou, V., Dumas, R., Cohen-Addad, C., Douce, R., Job, D., and Pebay-Peyroula, E. (1997) The crystal structure of plant acetohydroxy acid isomeroreductase complexed with NADPH, two magnesium ions, and a herbicidal transition state analog determined to 1.65 Å resolution, *EMBO J. 16*, 3405−3415.
30. Samuel, J., Luo, Y., Morgan, P. M., Strynadka, N. C. J., and Tanner, M. E. (2001) Catalysis and binding in L-ribulose-5-phosphate 4-epimerase: A comparison with L-fuculose-1-phosphate aldolase, *Biochemistry 40*, 14772−14780.
31. Lee, L. V., Vu, M. V., and Cleland, W. W. (2000) ^{13}C and deuterium isotope effects suggest an aldol cleavage mechanism for L-ribulose-5-phosphate 4-epimerase, *Biochemistry 39*, 4808−4820.
32. Lee, J. E., Poyner, R. R., Vu, M. V., and Cleland, W. W. (2000) Role of metal ions in the reaction catalyzed by L-ribulose-5-phosphate 4-epimerase, *Biochemistry 39*, 4821−4830.
33. Levy, G. C., Cargioli, J. D., and Racela, W. (1970) Nuclear magnetic resonance determination of ketone basicity and the use of ketones as indicators for the evaluation of medium acidity, *J. Am. Chem. Soc. 92*, 6238−6246.
34. Suhnel, J., and Schowen, R. L. (1991) In *Enzyme Mechanism from Isotope Effects* (Cook, P. F., Ed.) pp 3−35, CRC Press, Boca Raton, FL.
35. Argyrou, A., and Blanchard, J. S. (2004) Kinetic and chemical mechanism of *Mycobacterium tuberculosis* 1-deoxy-D-xylulose-5-phosphate isomeroreductase, *Biochemistry 43*, 4375−4384.

BI047312P